DC Load and Batteries Control Limitations for Photovoltaic Systems. Experimental Validation

Fabrice Locment, *Member, IEEE*, Manuela Sechilariu, *Member, IEEE*, and Issam Houssamo, *Student Member, IEEE*

***Abstract*—This study first presents an experimental control strategy of photovoltaic (PV) system composed of: PV array, dc–dc power converters, electrolytic storage, and programmable dc electronic load. This control aims to extract maximum power from PV array and manages the power transfer through the dc load, respecting the available storage level. The designed system allows simultaneously the supply of a dc load and the charge or the discharge of the storage during the PV power production. The experimental results obtained with a dSPACE 1103 controller board show that the PV stand-alone system responds within certain limits that appear as soon as one of the storage thresholds is reached: either loss of energy produced, or insufficient energy toward the load. In urban area, it is proposed to overcome these limitations by connecting the utility grid with the PV system while maintaining the priority for self-feeding. The experimental results of this PV semi-isolated system are shown and discussed. For this first approach, the goal was to verify the technical feasibility of the suggested system controls. The final results are energetically relevant.**

***Index Terms*—AC–DC power converters, batteries, dc–dc power converters, maximum power point tracking (MPPT), photovoltaic (PV) power system, power grid, power system control.**

I. Introduction

PHOTOVOLTAIC (PV) systems convert directly solar energy into electricity. Nowadays, the favorable politico-economic context allows a significant development of small means of decentralized PV power production, therefore, associated or integrated to buildings. PV power purchase conditions lead quite naturally these applications to grid-connected system with a total and permanent energy injection. Thus, currently, the PV grid-connected system is suggested in the most applications. There are many studies performed on different problems of PV grid-connected systems [1]–[5].

However, this development can lead to grid-connection incidents that become true technical constraints (setting voltage and frequency, islanding detection, etc.) [6].

In contrast, the other operating mode is the PV stand-alone system whose applications context is specific to the countryside or isolated locations. This system is seen as a substitute of utility grid connection. Given the intermittent PV production, the major problem associated with this system is the service continuity, whence the importance of energy storage and the addition of conventional sources, most often microturbines and cogeneration plant. The studies in this axis concentrate more on techno-economic feasibility conditions, optimized storage sizing, and load management [7]–[11].

The energy produced by a PV stand-alone system is intended for self-feeding, whence the isolated aspect. In order to obtain a reliable power distribution, this system needs to be secured by means of storage and/or conventional power production. Actually, passive houses strongly insulated and fully electrified, equipped with PV sources, could progressively become net-zero energy with significantly reduced greenhouse gas emissions. PV stand-alone system with adequate storage could cover the energy needs. Regarding house electrical loads, in order to obtain better energy efficiency, it is possible to supply electrical loads directly with dc power, whose realization is not trivial but nowadays technically feasible, and most often used in aerospace and naval applications. Regarding the protection devices, a panel of choice is possible, between the solid-state circuit breaker and the hybrid breaker, and permit, following the place and the purpose of the protection, to take the good switchgear in accordance with the specification of breaking time, perturbation on the bus, etc. These convergent factors have led to researches on dc power supply for buildings [4], [12], [13].

Taking into account this context, this paper focuses on the analysis of a PV stand-alone system control strategy and gives the system limits, then exposes a possible extension of the PV system. First, the PV system is presented: a PV array, dc–dc converters, electrolytic storage cells, and a programmable dc electronic load, which imposes currents in order to simulate the functioning of a low-consumption house lighting. In order to transfer to the load, at every moment, the maximum PV power available, a maximum power point tracking (MPPT) strategy is introduced. To feed correctly the dc load, the dc bus voltage is secured thanks to the storage system within the respect of the available storage level. The experimental results show that the system responds within certain limits that appear as soon as one of the storage voltage limits is reached. To overcome these limitations, the solution could be to connect the utility grid to the system, economically feasible in urban areas. Nevertheless, the produced PV power remains priority for self-feeding. The experimental results of this semi-isolated PV grid connected system are energetically relevant and show the technical feasibility.

II. PV Stand-Alone System

PV systems operating in a stand-alone mode consist of a PV source, storage means, ac or ac consumers and power

Manuscript received April 14, 2011; revised June 23, 2011, September 2, 2011, and December 8, 2011; accepted February 13, 2012. Date of current version May 15, 2012. Recommended for publication by Associate Editor L. Chang.

The authors are with the University of Technology of Compiegne, 60203 Compiegne, France (e-mail: fabrice.locment@utc.fr; manuela.sechilariu@utc.fr; issam.houssamo@utc.fr).

Color versions of one or more of the figures in this paper are available online at http://ieeexplore.ieee.org.

Digital Object Identifier 10.1109/TPEL.2012.2189134

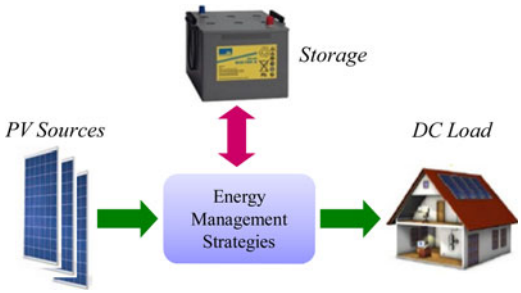

Fig. 1. PV stand-alone system power generation.

conditioning devices. Per definition, a PV stand-alone system involves no interaction with a utility grid. In almost all commercial PV stand-alone systems the only existing control is the batteries charge regulator. Compared to these systems, the suggested PV stand-alone system has a control that allows simultaneously the supply of a dc load and charge/discharge of the storage during the PV power production, as presented in [14].

A. System Overview

The PV stand-alone system is suggested for local dc generation that feed directly a dc load, in a safety configuration. This system extracts maximum power from PV sources and manages the power transfer through the dc load (house), respecting the available storage level and taking into account the requested load power, as illustrated in the Fig. 1. When the solar irradiation is too weak to generate the entire necessary power to transfer to the load, the dc load is supplied simultaneously by the PV system and the storage. In contrast, when the generated PV power is higher than the dc load requirements, and the storage has not a full state of charge (SOC), the system sends power back to the storage.

Aiming to optimize energy transfer, an experimental platform has been installed in the Centre Pierre Guillaumat of our university, whose images are given in Fig. 2. It refers mainly to 16 PV panels [2 kWp, Fig. 2(a)], a weather station, a set of electrolytic accumulators (Sonnenschein Solar S12/130 A, 12 V–130 Ah), a dSPACE 1103 controller board, and power electronic necessary devices (SEMIKRON SKM100GB063D, 600 V–100 A).

This system is associated with a programmable dc electronic load (Chroma 63202, 2.6 kW 500 V–50 A) that has a role to absorb and dissipate energy, allowing the simulation of the power required by the virtual house lighting.

B. PV Array

The PV array (*PVA*) is composed of 16 PV panels Solar Fabrik SF-130/2-125, whose electrical specifications are presented in Table I. The electrical coupling is given in the Fig. 3 with D reverse-current protection diodes and R_{LIG} power line losses resistances.

C. PV Stand-Alone System Electrical Scheme

The electrical scheme of PV stand-alone system consists of PVA, two-leg power converter (B_1 and B_2), electrolytic storage

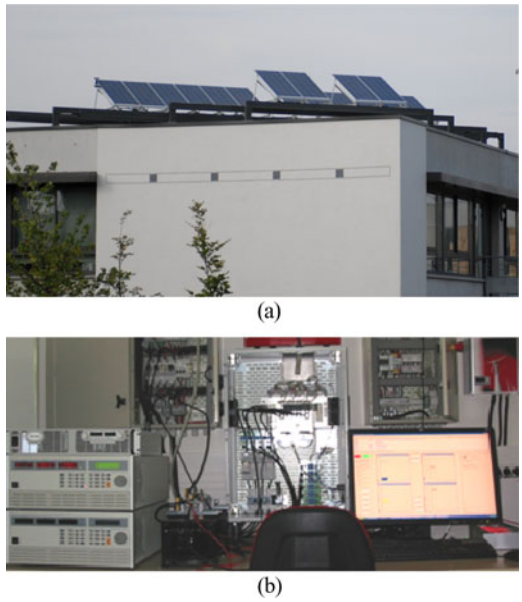

Fig. 2. (a) Image of PV array and (b) programmable dc electronic load and control devices.

TABLE I
ELECTRICAL STC SPECIFICATIONS OF PV PANEL

Solar-Fabrik SF-130/2-125	
N_S number of cells in series	36
I_{SC} short-circuit current (A)	7.84
V_{OC} open-circuit voltage (V)	21.53
I_{MPP} maximum power point current (A)	7.14
V_{MPP} maximum power point voltage (V)	17.50
K_0 temperature coefficient for current (A/K)	0.00545
θ^* temperature reference (K)	298.15
g^* solar irradiance reference (W/m^2)	1000

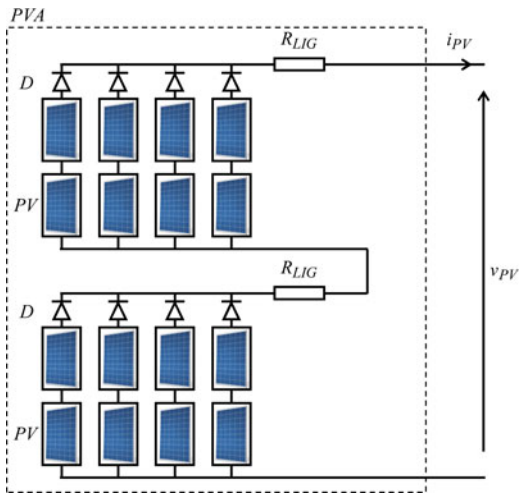

Fig. 3. PVA electrical coupling.

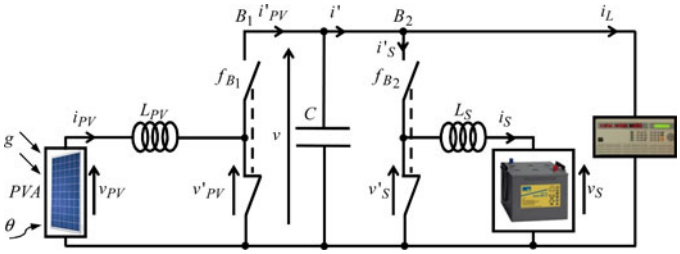

Fig. 4. PV stand-alone system electrical scheme.

TABLE II
NOTATION OF VARIABLES

Symbol notation	
Reference variable	x^*
Modulated variable	x'
Reference and modulated variable	x'^*

cells, programmable dc electronic load and a set of inductors and capacitor in order to ensure compatibility between the different elements. Inductors and capacitor used in the experimental setup were designed to obtain a very large time constant (of the order of a few seconds). Taking into account the technical conditions available (PV panels wiring, converter structure, etc.), this study is assumed to be primarily energy transfer study rather than the control study. In this context, the designed electrical scheme of stand-alone PV is shown in the Fig. 4, where g and θ are, respectively, solar irradiance and PV cells temperature.

In this paper, the notation of variables is done following the Table II.

In order to extract the maximum power of PVA, an impedance adapter is used. It consists of $L_{\rm PV}$ inductor, C capacitor, and B_1 power converter leg. The C capacitor is a common element for PVA and storage system.

The described PVA and impedance adapter subsystem are modeled as follows

$$\frac{di_{\rm PV}}{dt} = \frac{1}{L_{\rm PV}}\left(v_{\rm PV} - v'_{\rm PV}\right)$$
$$\begin{bmatrix} i'_{\rm PV} \\ v'_{\rm PV} \end{bmatrix} = a_{\rm PV}\begin{bmatrix} i_{\rm PV} \\ v \end{bmatrix}$$
$$a_{\rm PV} = \frac{1}{T}\int_0^T f_{B1}\,dt\; a_{\rm PV} \in [0;1]\,. \tag{1}$$

The dc bus consists of a C capacitor and an electrical coupling of v voltage. The operating dc bus equations are

$$\frac{dv}{dt} = \frac{1}{C}\left(i'_{\rm PV} - i'\right)$$
$$i' = i'_S + i_L\,. \tag{2}$$

The storage subsystem consists of a set of electrolytic storage cells. It is a matter of voltage source v_S, inductor L_S, capacitor C, and B_2 power converter leg. The dc bus voltage v is secured thanks to this subsystem. Equations (3) give storage system modeling equations

$$\frac{di_S}{dt} = \frac{1}{L_S}\left(v'_S - v_S\right)$$
$$\begin{bmatrix} i'_S \\ v'_S \end{bmatrix} = a_S\begin{bmatrix} i_S \\ v \end{bmatrix}$$
$$a_S = \frac{1}{T}\int_0^T f_{B2}\,dt\; a_S \in [0;1]\,. \tag{3}$$

The dc load is modeled like a current source i_L, which represents a lighting installation power demand. Thus, in this study case, for experimental test the programmable dc electronic load imposes currents in order to simulate the functioning of a low-consumption house's lighting.

D. Control System Strategy

The system control strategy is designed for two objectives: extract maximum power from PVA and manage the power transfer through the dc load with the respect to available storage level. By means of two settings, $a^*_{\rm PV}$ and a^*_S, a global control strategy is suggested. Thus, in order to extract the PVA maximum power, the incremental conductance (INC) MPPT strategy is suggested. In addition, the dc bus voltage must be secured respecting the available storage level.

1) Maximum Power Tracking Method: The power produced by PVA depends on the solar irradiance, PV cell temperature, array voltage and the current through the PVA. The operating point of a load connected at the PV generator does not coincide always with the optimal point and varies according to the weather conditions. In order to maximize the produced energy from the PVA, an MPPT method is needed to find and maintain the peak power. Many MPPT methods have been suggested and reported in the literature [15]–[18].

Two direct algorithms are commonly used to track the maximum power point (MPP): the perturb and observe (P&O) method and INC method. They act in real time on the voltage reference variable, corresponding to the maximum power provided by the PV system. In [19], these two algorithms, subject of an experimental comparison, impose the current reference. According to this study, the experimental measures, obtained for strictly the same given set of conditions, show that both MPPT energy efficiencies of the suggested algorithms are very similar.

Generally, the difference observed between the extracted powers on the basis of these two algorithms is negligible for a period of at least a day. A real difference between the extracted powers can be observed for very short periods, up to the second. Depending specially on solar irradiance variations (period and amplitude), an algorithm may be better for an instant measured power but without necessarily a satisfactory time response. In terms of energy, for a significant period, this difference becomes negligible. It is well known that a PV system becomes interesting for an energy production that requires a significant period of time (day, week). Nevertheless, in the long term, INC algorithm can extract a little more energy available from the PVA with a better performance: rapid time response to solar irradiance

variations and less oscillations around the MPP. In this case, the INC algorithm could be rather preferred to P&O algorithm.

The MPPT strategy aims to find in real time the voltage or current reference for which PV panel would provide the maximum output power. In this study, we are interested to INC MPPT algorithm that is implemented in order to impose the current reference $i^*_{\rm PV}$. According to the available equipment, this choice was made to avoid an overly complex control (nested loops, pole placement, etc.) and the addition of a capacitor.

Hence, the derivate of the PVA impedance $dv_{\rm PV}/di_{\rm PV}$ is introduced. It is because the slope tangent of the characteristic $p_{\rm PV} = f\left(i_{\rm PV}\right)$ (with $p_{\rm PV} = v_{\rm PV}\ i_{\rm PV}$) is zero in MPP, positive on the MPP left side, and negative on the MPP right side. As the power is equal to the product of current and voltage, the calculation of this slope is given as follows:

$$\frac{dp_{\rm PV}}{di_{\rm PV}} = v_{\rm PV} + i_{\rm PV}\frac{dv_{\rm PV}}{di_{\rm PV}}. \tag{4}$$

The following equationgives the development of this derivate in MPP

$$\frac{v_{\rm PV}}{i_{\rm PV}} + \frac{dv_{\rm PV}}{di_{\rm PV}} = 0. \tag{5}$$

When the operating point is to the left of the MPP, there is $\left(v_{\rm PV}/i_{\rm PV}\right) + \left(dv_{\rm PV}/di_{\rm PV}\right) > 0$, whereas when the operating point is to the right of the MPP, there is $\left(v_{\rm PV}/i_{\rm PV}\right) + \left(dv_{\rm PV}/di_{\rm PV}\right) < 0$

$$\begin{aligned} di_{\rm PV} &\approx \Delta i_{\rm PV} = i_{\rm PV}\left(z\right) - i_{\rm PV}\left(z-1\right) \\ dv_{\rm PV} &\approx \Delta v_{\rm PV} = v_{\rm PV}\left(z\right) - v_{\rm PV}\left(z-1\right). \end{aligned} \tag{6}$$

From the instantaneous measurement of $i_{\rm PV}$ and $v_{\rm PV}$, and assuming (6) with z and $z-1$ instants measurement, the algorithm can instantly calculate $v_{\rm PV}/i_{\rm PV}$ and $dv_{\rm PV}/di_{\rm PV}$ to deduct the direction of perturbation leading to the MPP. This is done by acting on $i^*_{\rm PV}$. Fig. 5 shows the flowchart of this version of the INC algorithm.

Fig. 6 shows the INC MPPT strategy experimental result and proves that the algorithm works correctly according to $i_{\rm PV}$ proportional to g, with solar irradiation and PVA current recorded on 6th April, 2011 in Compiegne, France.

The reference current $i^*_{\rm PV}$ is obtained following the INC MPPT strategy. The adopted control is performed according to $a^*_{\rm PV}$ setting described as follows:

$$a^*_{\rm PV} = \frac{-C_{\rm PV}\left(i^*_{\rm PV} - i_{\rm PV}\right) + v_{\rm PV}}{v}. \tag{7}$$

The $C_{\rm PV}$ controller used in (7) is proportional, with a very wide bandwidth. As the inductors and capacitor used in the experimental setup were designed to obtain a very large time constant (of the order of a few seconds), the synthesis of controllers was performed based on pure integrator instead of a first-order integrator. Thus, in order to simplify the control, in this study, all controllers are proportional with disturbances compensation.

2) Batteries and DC Load Control: In order to feed correctly the dc load, the dc bus voltage must be secured respecting the available storage level. In this case, with C_S controller, the

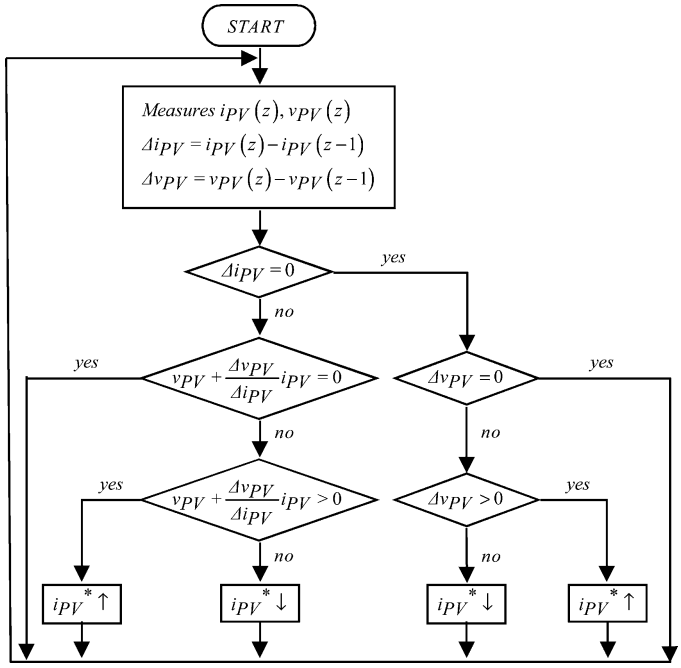

Fig. 5. Flowchart of the INC algorithm.

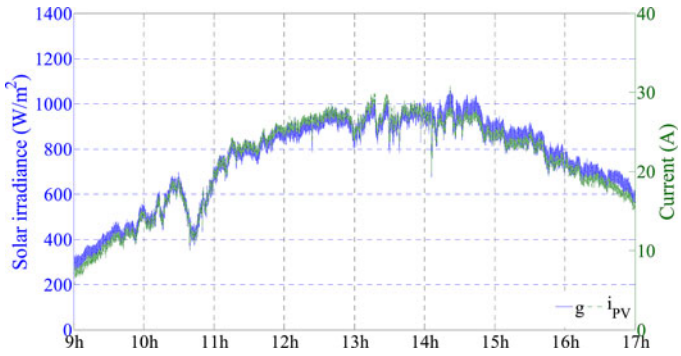

Fig. 6. Experimental result with INC algorithm.

following setting is used

$$a^*_S = \frac{C_S\left(i^*_S - i_S\right) + v_S}{v}. \tag{8}$$

The current reference i^*_S is determined with a v control loop and a power balance. By inverting (2), with C_V controller, the current reference i'^* is equal to

$$\begin{aligned} i'^* &= -C_V\left(v^* - v\right) + i'_{\rm PV} \\ i'^*_S + i_L &= -C_V\left(v^* - v\right) + i'_{\rm PV}. \end{aligned} \tag{9}$$

According to the assumption that there are not losses through the inductors L_S, with $v\ i'^*_S = v_S\ i^*_S$, and $L_{\rm PV}$, with $v\ i'_{\rm PV} = v_{\rm PV}\ i_{\rm PV}$, and neglecting the total losses of power converter legs (B_1 and B_2), the product of (9) by v gives

$$i^*_S = \frac{1}{v_S}\left(v\left(-C_V\left(v^* - v\right) - i_L\right) + v_{\rm PV}\ i_{\rm PV}\right). \tag{10}$$

The control diagram for the dc bus voltage for PV stand-alone system is illustrated in Fig. 7. The voltage $v_{\rm CR}$ is a carrier

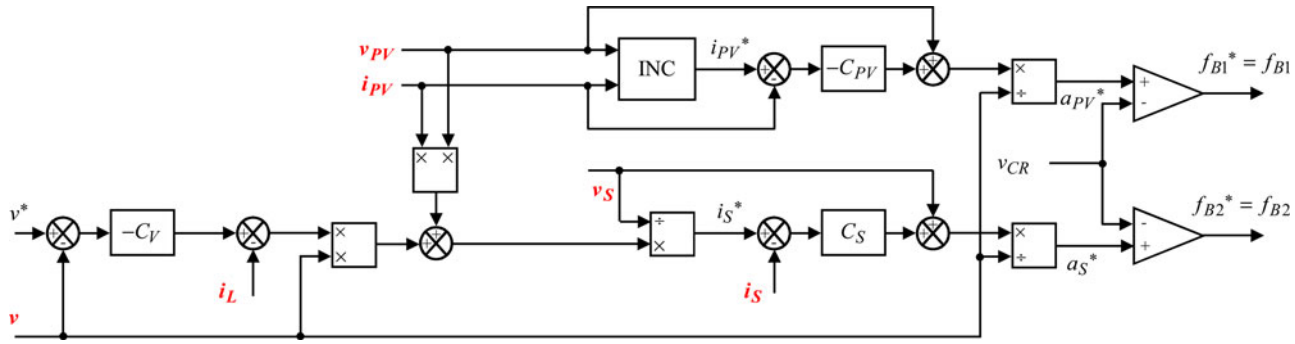

Fig. 7. Control diagram for the dc bus voltage for PV stand-alone system.

reference needed to achieve pulsewidth modulation. Fig. 7 shows that the only control variable is v^* with six measurable variables (v, i_L, $v_{\rm PV}$, $i_{\rm PV}$, v_S, and i_S).

E. Experimental Results Analysis

The goal of this study is more to validate a comprehensive approach rather than purely numerical results. For this reason, we do not give the numerical values of various system components studied. All the implemented automatic controls, described earlier, are working satisfactorily. The experimental results of the PV stand-alone system are presented in Figs. 8 and 9. For a solar irradiance g and a cell temperature θ corresponding to an arbitrary day, 6th April, 2011 in Compiegne, France, as illustrated in Fig. 8(a), the powers evolutions are shown in Fig. 8(b). The following powers expressions are used: $p_{\rm LOAD} = vi_L$ power absorbed by lighting installation, $p_{\rm PV} = v_{\rm PV}\, i_{\rm PV}$ power supplied by PVA, $p_S = v_S\, i_S$ storage system transfer power and $\Delta p = p_{\rm LOAD} - p_{\rm PV}$.

Concerning the theoretical lighting power evolution $p_{\rm LOAD}$, as illustrated in Fig. 8(b), it is considered an idealized arbitrary power required by the load.

Fig. 9 illustrates the storage voltage evolution v_S, as well as the current crossing i_S. Figs. 8(b) and 9 show that for $\Delta p < 0$ the storage system receives energy, in contrast for $\Delta p > 0$ it provides.

For the period taken into account, these results show that in the limit of the storage (115.2 V as maximum voltage and 81.6 V as minimum voltage, constructor datasheets), and whatever the sign and the amplitude of the difference of Δp, this experimental system is secured.

Regarding the dc bus, it is shown in Fig. 10 that the voltage remains at an almost constant level. The dc bus stability is satisfactory with voltage's fluctuation less than 1.25%. These fluctuations can be improved by means of a better control.

Finally, for the period taken into account, the system responds satisfactory, but note that once the storage has reached its high or low voltage limits, the system could lead to either loss of energy produced, or insufficient energy toward the load. Thus, the implementation of an algorithm able to extract a PV limited power according to the load request and to manage the load shedding is needed. In addition, the PV stand-alone system involves an optimized sizing adapted to each specific load and according its specific use. The sizing's problem could be overcome if the

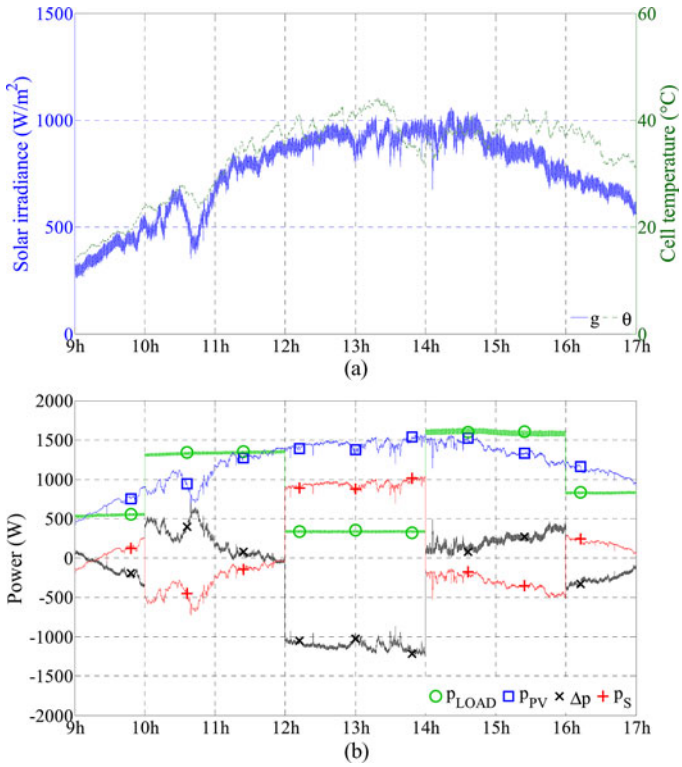

Fig. 8. Evolutions of : (a) Solar irradiance and cell temperature and (b) powers for PV stand-alone system.

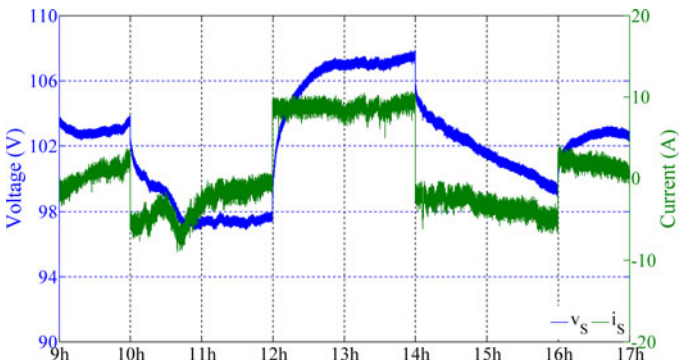

Fig. 9. Evolution of storage voltage v_S and storage current i_S for PV stand-alone system.

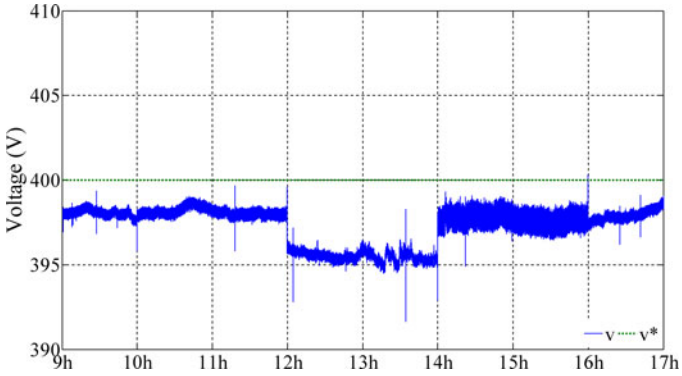

Fig. 10. Evolution of dc bus voltage for PV stand-alone system.

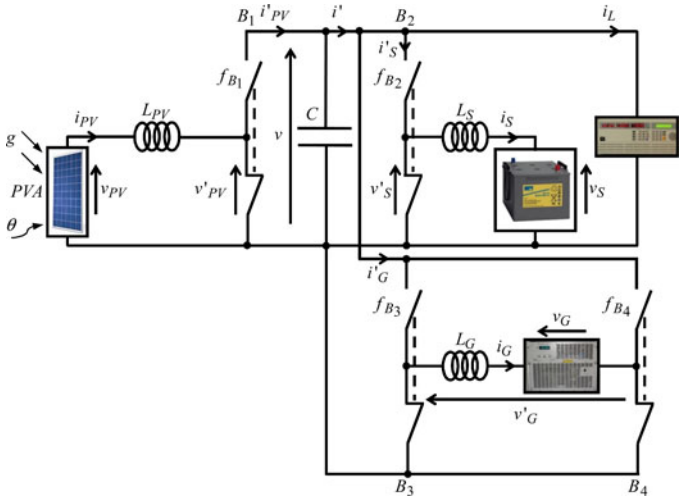

Fig. 11. PV semi-isolated system electrical scheme.

utility grid connection may be economically made. This is why, in urban areas, the utility grid connection is desirable within a PV system, and gives a really continuity power service. Therefore, as soon as one of the storage SOC thresholds is reached the utility grid takes over, as presented in the next section.

III. PV Semi-Isolated System

A PV system in semi-isolated and safety grid configuration for local generation is suggested. The energy produced remains priority for self-feeding. Regarding this system, satisfactorily simulation results have been presented in [20].

A. PV Semi-Isolated System Electrical Scheme

The electrical scheme of PV semi-isolated system is presented in the Fig. 11. The reference current i^*_{PV} is obtained following the INC MPPT strategy described earlier. The PV semi-isolated system operates respecting the available storage level and taking into account the utility grid connection. In case of insufficient energy toward the load, the system security is ensured thanks to the grid-connection and by means of minimized storage, which is primarily involved in smoothing of the requested power. If any excess PV power, the grid-connection gives the possibility to trade it back.

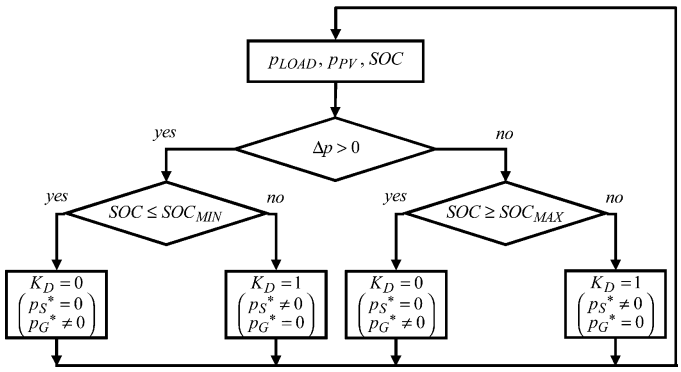

Fig. 12. PV semi-isolated system flowchart strategy.

In order to be economically profitable, and therefore able to continue the use of already existing cable infrastructure (400/230 V ac) for house lighting, an optimal dc bus voltage value to adopt may be 325 $\mathrm{V_{DC}}$ [12], [21]. This techno-economic compromise leads to test the suggested PV semi-isolated system for this value. Nevertheless, for technical reasons, in this study we adopt for the dc bus voltage the value of 400 $\mathrm{V_{DC}}$. Taking into account calculations of losses and power transfer rate, as presented in [21], this voltage value achieves better energy efficiency in a quantitative comparison of high efficiency ac versus dc. Regarding the voltage limits of the cable infrastructure used in building, the value of 400 $\mathrm{V_{DC}}$ is adequate.

Experimental PV semi-isolated system refers to the same 16 PV panels, weather station, electrolytic accumulators, and programmable dc electronic load that allow the simulation of the lighting power. The utility grid emulator (linear amplifier 3 kV·A) is electrically coupled to the dc isolated network through the B_3 and B_4 power converter legs and the L_G inductor and C capacitor.

In this configuration of PV semi-isolated system, (1) to (8) remain valid with the following change of the current equation:

$$i' = i'_S + i_L + i'_G. \tag{11}$$

The utility grid emulator operating equations are

$$\begin{aligned} \frac{di_G}{dt} &= \frac{1}{L_G}\left(v'_G - v_G\right) \\ \begin{bmatrix} i'_G \\ v'_G \end{bmatrix} &= a_G \begin{bmatrix} i_G \\ v \end{bmatrix} \\ a_G &= \frac{1}{T}\int_0^T \left(f_{B3} - f_{B4}\right) dt, f_{B3} = \overline{f_{B4}}, a_G \in [-1;1]. \end{aligned} \tag{12}$$

Regarding the grid synchronization, a method suitable for grid-connected converters based on a phase-locked loop is used [22]. Furthermore, to simplify this study, it is assumed that no reactive power can be supplied or absorbed by the grid: i_G is always in phase or opposite-phase with v_G.

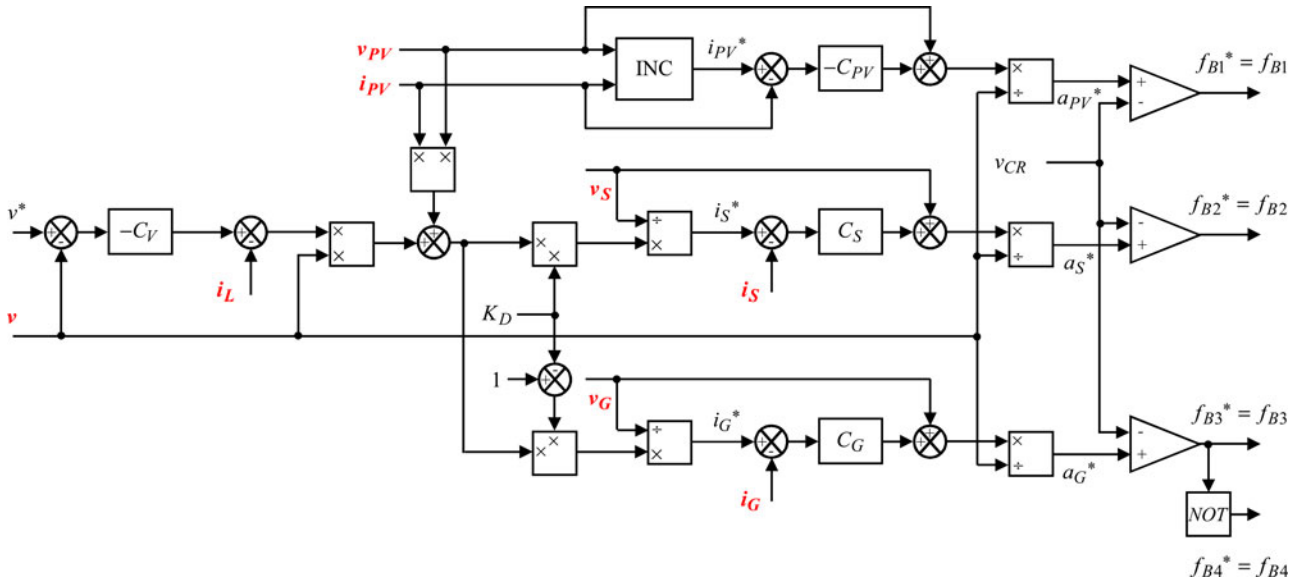

Fig. 13. Control diagram for the dc bus voltage for PV semi-isolated system.

B. Control System Strategy

In order to control four state variables ($i_{\rm PV}$, v, i_S and i_G), in addition to the previously defined settings $a^*_{\rm PV}$ and a^*_S, a third setting a^*_G is introduced by (13). The C_G controller is proportional (taking into account the same reasons as mentioned earlier), with a very wide bandwidth

$$a^*_G = \frac{C_G\,(i^*_G - i_G) + v_G}{v}. \tag{13}$$

The security system is exactly achieved by dc bus voltage control. The dc bus current adjustment i^* is defined by

$$i'^* = -C_V\,(v^* - v) + i'_{\rm PV} \tag{14}$$

where C_V is the same corrector like $C_{\rm PV}$, C_S, and C_G, with the same type of setting.

From (11) and (14), the following expression is obtained:

$$i'^*_S + i'^*_G = -C_V\,(v^* - v) + i'_{\rm PV} - i_L. \tag{15}$$

According to the assumption that there are not losses through the inductors L_G and neglecting the total losses of power converter legs (B_3 and B_4) with $v\ i'^*_G = v_G\ i^*_G$, the product of (15) by v gives

$$v_S\ i^*_S + v_G\ i^*_G = v\,(-C_V\,(v^* - v) - i_L) + v_{\rm PV}\ i_{\rm PV}. \tag{16}$$

DC load, that represents house lighting, imposes the values of voltage v^* (400 $\rm V_{DC}$) and the current i_L. Therefore, in this case, the combination of these two powers ($v_S\ i^*_S + v_G\ i^*_G$) involves the regulation and the security system. Using the values of this combination, an infinite number of solutions may exist. In this study, a simple and quick to implement strategy is applied. This strategy was not necessarily developed to improve global efficiency or life cycle of the storage system. For this first approach, the goal is to verify the feasibility of the PV semi-isolated system control. The suggested strategy gives priority to the storage charge or discharge before the use of the utility grid without allowing their use simultaneously. Thus, a distribution coefficient K_D is applied. In this experimental test, only two values are retained, $K_D = 0$ and $K_D = 1$, but further work involves more elaborate strategies and therefore a multitude of possible K_D values. Equation (16) becomes

$$\begin{aligned} &K_D\ v_S\ i^*_S + (1 - K_D)\ v_G\ i^*_G \\ &\quad = v\,(-C_V\,(v^* - v) - i_L) + v_{\rm PV}\ i_{\rm PV}. \end{aligned} \tag{17}$$

Fig. 12 shows flowchart of the applied strategy with $\rm SOC_{MAX}$ and $\rm SOC_{MIN}$ the limits high and respectively low of SOC.

The control diagram for the dc bus voltage for the suggested PV semi-isolated system is illustrated in Fig. 13.

C. Experimental Results Analysis

The experimental test was recorded on 10th April, 2011 in Compiegne, France. The results are given in Fig. 14 using $p_G = v_G\ i_G$ as utility grid transfer power. For the period taken into account, we observe that the strategy outlined earlier is well respected. For $\Delta p < 0$ the storage system receives energy, in contrast it provides. The storage charge discharge operation has priority over the utility grid. Once the battery has reached its limits high or low, $\rm SOC_{MAX}$ or $\rm SOC_{MIN}$, the public grid takes over.

The storage SOC and K_D distribution coefficient evolutions are given in Fig. 15. Therefore, as soon as one of the storage SOC thresholds is reached the utility grid takes over. The evolution of distribution coefficient K_D shows this change. Regarding the constraint to record a significant period related to K_D changes, the storage SOC thresholds were arbitrary imposed as: $\rm SOC_{MIN} = 48\%$ and $\rm SOC_{MAX} = 55\%$.

Fig. 16 shows the charge and discharge storage cycle following the storage current i_S sign and the storage voltage evolution. The storage hysteresis effect can be seen during the period taken into account. Following a charge operation, the storage voltage

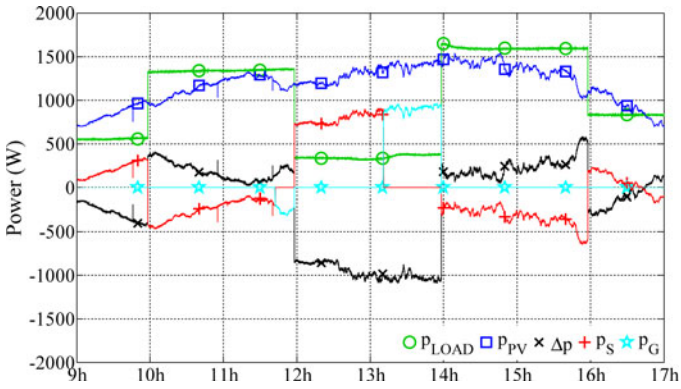

Fig. 14. Evolutions of powers of PV semi-isolated system.

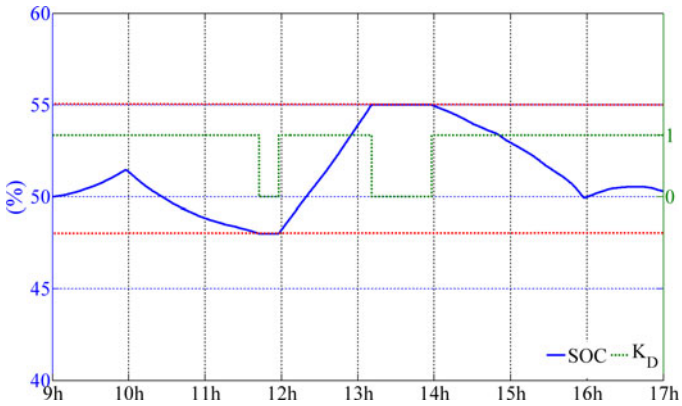

Fig. 15. Evolution of SOC and distribution coefficient K_D for PV semi-isolated system.

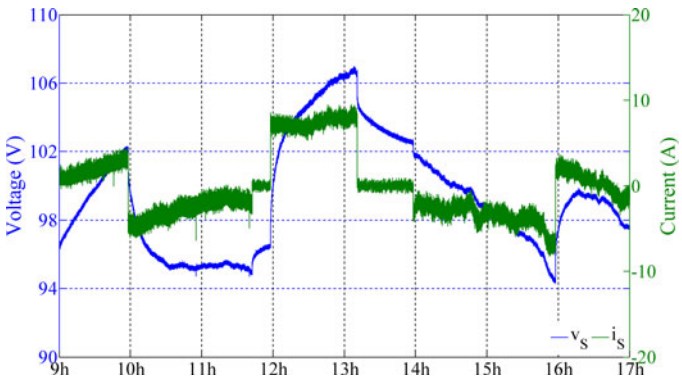

Fig. 16. Evolution of storage voltage v_S and storage current i_S for PV semi-isolated system.

relaxes to a value less than the true open-circuit voltage corresponding to its SOC.

Taking into account that the goal was to verify the feasibility of the suggested system control, finally, we can say that the overall PV semi-isolated system, as has been modeled, responds satisfactorily within the outlined strategy. However, in order to use fully and correctly the available storage, its control must be improved. In addition, in our further work, K_D binary values will be replaced by calculated values corresponding to techno-economic criteria, weather, conditions of use, forecast power demand, etc.

IV. Conclusion

Autonomous systems of local renewable power production become increasingly complex and selective for many powered loads. In this paper, first, an experimental PV stand-alone system control strategy was presented and its limits were discussed. These results show that the system allows simultaneously supply of a dc load and the charge or the discharge of the storage during the PV power production. Nevertheless, it responds within certain limits of the storage SOC thresholds. Obtained result indicates that the suggested method operates successfully within the control of a PV stand-alone system but involves an optimized storage sizing and an algorithm able to extract a PV limited power according to the load request and to manage the load shedding.

In order to overcome limits, it is shown that a PV semi-isolated system can be applied in urban areas. This second PV system uses a utility grid connection, which is economically made in urban areas. The experimental results show that the PV semi-isolated system responds within certain limits of the PV power and utility grid availability.

In this study, a simple and quick control to implement was done for both PV systems, stand-alone system and semi-isolated system. These controls were not necessarily developed to improve global energy efficiency. For this first approach, the goal was to verify the feasibility of the suggested system controls. The proposed PV system (stand-alone and on-grid) could run successfully for small building and/or house, but the economic criterion remains the main problem. Technical solutions exist, but certainly not yet ready to plug and play. However, the result of this paper leads to study, design, and develop an intelligent energy management system, which optimizes the power transfer within a multi-source power system. The chosen approach will take into account the uncertainties on PV power production, utility grid availability, load request, and load shedding, in order to achieve more efficient power transfer with a minimized public grid impact. The main work is a multicriteria optimization that is related to the risk of discrepancy between prediction, planning and actual operation, on the one hand, and the need to take into account criteria, constraints and indicators (comfort level, meteorological data, life cycle, sustainable operating conditions, etc.) difficult to quantify, on the other hand.

References

[1] L. Zhang, K. Sun, Y. Xing, L. Feng, and H. Ge, "A modular grid-connected photovoltaic generation system based on DC bus," *IEEE Trans. Power Electron.*, vol. 26, no. 2, pp. 523–531, Feb. 2011.

[2] B. Yang, W. Li, Y. Zhao, and X. He, "Design and analysis of a grid-connected photovoltaic power system," *IEEE Trans. Power Electron.*, vol. 25, no. 4, pp. 992–1000, Apr. 2010.

[3] J. L. Agorreta, M. Borrega, J. Lopez, and L. Marroyo, "Modeling and control of N-paralleled grid-connected inverters with LCL filter coupled due to grid impedance in PV plants," *IEEE Trans. Power Electron.*, vol. 26, no. 3, pp. 770–785, Mar. 2011.

[4] Z. Zhang, M. Chen, M. Gao, Q. Mo, and Z. Qian, "An optimal control method for grid-connected photovoltaic micro-inverter to improve the efficiency at light-load condition," in *Proc. IEEE Energy Convers. Congr. Expo.*, [CD-ROM], 2011, pp. 219–224.

[5] Y.-M. Chen, H.-C. Wu, Y.-C. Chen, K.-Y. Lee, and S.-S. Shyu, "The AC line current regulation strategy for the grid-connected PV system," *IEEE Trans. Power Electron.*, vol. 25, no. 1, pp. 209–218, Jan. 2010.

[6] F. Blaabjerg, R. Teodorescu, M. Liserre, and A. V. Timbus, "Overview of control and grid synchronization for distributed power generation systems," *IEEE Trans. Ind. Electron.*, vol. 53, no. 5, pp. 1398–1409, Oct. 2006.
[7] M. Kolhe, "Techno-economic optimum sizing of a stand-alone solar photovoltaic system," *IEEE Trans. Energy Convers.*, vol. 24, no. 2, pp. 511–519, Jun. 2009.
[8] M. Benghanem, "Low cost management for photovoltaic system in isolated site with new IV characterization model proposed," *Energy Convers. Manage.*, vol. 50, pp. 748–755, 2009.
[9] M. J. V. Vazquez, J. M. A. Marquez, and F. S. Manzano, "A methodology for optimizing stand-alone PV-system size using parallel-connected DC/DC converters," *IEEE Trans. Ind. Electron.*, vol. 55, no. 7, pp. 2664–2673, Jul. 2008.
[10] D. D. Lu and V. G. Agelidis, "Photovoltaic-battery-powered DC bus system for common portable electronic devices," *IEEE Trans. Power Electron.*, vol. 24, no. 3, pp. 849–855, Mar. 2009.
[11] R. J. Wai, W. H. Wang, and C. Y. Lin, "High-performance stand-alone photovoltaic generation system," *IEEE Trans. Ind. Electron.*, vol. 5, no. 1, pp. 240–250, Jan. 2008.
[12] D. Salomonsson and A. Sannino, "Low-voltage DC distribution system for commercial power systems with sensitive electronic loads," *IEEE Trans. Power Deliv.*, vol. 22, no. 3, pp. 1620–1627, Jul. 2007.
[13] B. Liu, S. Duan, and T. Cai, "Photovoltaic DC-building-module-based BIPV system—Concept and design considerations," *IEEE Trans. Power Electron.*, vol. 26, no. 5, pp. 1418–1429, May 2011.
[14] F. Locment, M. Sechilariu, and I. Houssamo, "Batteries and DC charge control of stand-alone photovoltaic system. Experimental validation," in *Proc. 14th Int. Power Electron. Motion Control Conf. EPE [CD-ROM]*, 2010, pp. T12-43–T12-48.
[15] A. K. Abdelsalam, A. M. Massoud, S. Ahmed, and P. N. Enjeti, "High-performance adaptive perturb and observe MPPT technique for photovoltaic-based microgrids," *IEEE Trans. Power Electron.*, vol. 26, no. 4, pp. 1010–1021, Apr. 2011.
[16] Y. H. Ji, D. Y. Jung, J. G. Kim, J. H. Kim, T. W. Lee, and C. Y. Won, "A real maximum power point tracking method for mismatching compensation in PV array under partially shaded conditions," *IEEE Trans. Power Electron.*, vol. 26, no. 4, pp. 1001–1009, Apr. 2011.
[17] B. N. Alajmi, K. H. Ahmed, S. J. Finney, and B. W. Williams, "Fuzzy-logic-control approach of a modified hill-climbing method for maximum power point in microgrid standalone photovoltaic system," *IEEE Trans. Power Electron.*, vol. 26, no. 4, pp. 1022–1030, Apr. 2011.
[18] S. L. Brunton, C. W. Rowley, S. R. Kulkarni, and C. Clarkson, "Maximum power point tracking for photovoltaic optimization using ripple-based extremum seeking control," *IEEE Trans. Power Electron.*, vol. 25, no. 10, pp. 2531–2540, Oct. 2010.
[19] I. Houssamo, F. Locment, and M. Sechilariu, "Maximum power tracking for photovoltaic power system: Development and experimental comparison of two algorithms," *Renewable Energy*, vol. 35, no. 10, pp. 2381–2387, 2010.
[20] M. Sechilariu, F. Locment, and I. Houssamo, "Multi-source power generation system in semi-isolated and safety grid configuration for buildings," in *Proc. IEEE Mediterranean Electrotech. Conf. [CD-ROM]*, 2010.
[21] A. Sannino, G. Postiglione, and M. Bollen, "Feasibility of a DC network for commercial facilities," *IEEE Trans. Ind. Appl.*, vol. 39, no. 5, pp. 1499–1507, Sep. 2003.
[22] M. Ciobotaru, V. G. Agelidis, R. Teodorescu, and F. Blaabjerg, "Accurate and less-disturbing active antiislanding method based on PLL for grid-connected converters," *IEEE Trans. Power Electron.*, vol. 25, no. 6, pp. 1576–1584, Jun. 2010.

Fabrice Locment (M'11) received the Dipl.Ing. degree in electrical engineering from the Polytech' University of Lille, in 2003, and the M.S. and Ph.D. degrees in electrical engineering from University of Science and Technology of Lille, Lille, France, in 2003 and 2006, respectively.

From 2006 to 2008, he was a Researcher in post-doctoral position with Arts et Metiers ParisTech, and since 2008, an Associate Professor with the University of Compiegne, Compiegne, France. He has more than 25 papers published. His current research interests include designing, modeling, and control of electrical systems (particularly: polyphase machine, photovoltaic, and wind).

Manuela Sechilariu (M'11) received the Dipl.Ing. degree in electrical engineering from the Polytechnical University of Iasi, Iasi, Romania, in 1986, and the Ph.D. degree in electrical engineering and automatic from the University of Angers, Angers, France, in 1993.

From 1986 to 1988, she was with the Transducers and Direct Regulators Plant, Pascani, Romania, and then was with Polytechnical University of Iasi, where she was an Assistant Professor with the Electrical Engineering Department. In 1994, she was an Associate Professor with the Automated Systems Engineering Department, University of Angers, Angers, France. Since 2002, she has been with the University of Compiegne, Compiegne, France, where she is currently an Associate Professor. She has more than 45 papers published. Her areas of interests include renewable energy, smart grid, photovoltaic-powered systems, energy management, intelligent control, supervision, Petri Nets modeling.

Issam Houssamo (S'11) received the B.S. and M.S. degrees in electrical engineering from the University of Tichrine, Lattakia, Syria, in 2002 and 2003, respectively. He is currently working toward the Ph.D. degree at the University of Technology of Compiegne, Compiegne, France.

From 2003 to 2005, he was an Assistant Professor Electrical Engineering Department with the University of Tichrine. In 2007, he received the M.S. degree in electrical engineering from Ecole Centrale of Lyon, France. His current research interests include renewable energy systems, design of photovoltaic cells, and photovoltaic-powered systems.